Experimental Behavior of Steel Fixed Bearings and Implications for Seismic Bridge Response

J. S. Steelman, M.ASCE[1]; E. T. Filipov, S.M.ASCE[2]; L. A. Fahnestock, P.E., M.ASCE[3]; J. R. Revell, P.E.[4]; J. M. LaFave, P.E.[5]; J. F. Hajjar, P.E., F.ASCE[6]; and D. A. Foutch, P.E., M.ASCE[7]

Abstract: Steel fixed bearings are commonplace structural elements for transmitting loads from superstructures to substructures, and they have typically occupied a role of elastic force transfer elements within the overall scheme of an earthquake resisting system (ERS). Recent revisions to design and guide specifications have acknowledged the possibility of bearings acting as fuses, but there is little research available to characterize bearing behavior for such design roles or the associated bridge response to be expected when bearings have fused. One design approach, adopted by the Illinois DOT (IDOT), applies capacity design principles and permits the bearings and superstructure to slide on the substructure. The intent of this design approach is to capture some of the beneficial aspects of conventional isolated systems, such as period elongation, reduction of force demands, and protection of substructures from large inelastic displacement demands, without incurring the additional design provisions and fabrication costs to satisfy the requirements for seismic isolation systems. To achieve this quasi-isolated bridge response, steel fixed bearings are used as fusing elements, where the steel pintles or anchor rods rupture, and the fixed bearing plates become free to slide on the supporting pier cap. A properly proportioned bearing will fuse prior to superstructure/substructure elements experiencing inelastic demands. The University of Illinois has been collaborating with IDOT to investigate the behavior of quasi-isolated bridge systems and to calibrate and refine IDOT's ERS design and construction methodology. The research is composed of experimental testing to characterize fundamental bearing behavior, coupled with nonlinear global bridge modeling to evaluate limit state progression and estimate maximum displacement demands of the superstructure relative to the substructure. The cyclic response of full-scale steel low-profile fixed bearings demonstrates predictable sliding behavior, but based on current design procedures, these bearings are often overdesigned for use as fuses in quasi-isolated bridges. Consequently, a bridge, which in other respects may exhibit satisfactory quasi-isolated response, might also incur significant damage to the substructure unit where fixed bearings are provided. A parametric study of global bridge response demonstrates that the anchorage of fixed bearings to substructures could be reduced to limit the damage to the supporting substructure unit while incurring only a nominal increase in superstructure displacement demands. **DOI: 10.1061/(ASCE)BE.1943-5592.0000540.**

Author keywords: Highway bridges; Earthquake-resistant structures; Friction; Isolation; Cyclic tests; Nonlinear analysis; Nonlinear response; Fixed bearings; Quasi-isolation; Full-scale tests; Friction coefficient.

Introduction

Steel bearings are a historically commonplace means of transmitting loads from bridge superstructures to substructures, as both fixed and expansion bearings (Mander et al. 1996), although recent developments in bearing technologies have largely superseded steel expansion bearings so that steel bearings are now only recommended for use as fixed bearing types (AASHTO 2004). Design for gravity loads is straightforward, generally requiring only that the steel plates are capable in flexure of distributing the dead and live loads to concrete substructures without yielding the plates or crushing the concrete. Complications arise, however, when seismic demands are considered. As recently as 2007, Section 14.8.3.1 of the AASHTO LRFD bridge design specifications (AASHTO 2010b) required that "all girders shall be positively secured to supporting bearings by a connection that can resist the horizontal forces that may be imposed on it." However, in recent editions, this requirement has been appended by the caveat "unless fusing or irreparable damage is permitted at the extreme event limit state." Similarly, Section 7.9.1 of the AASHTO guide specifications for LRFD seismic bridge design (AASHTO 2011) includes a disclaimer that "structural fuse bearings are not addressed in these Guide Specifications."

Design guidance supported by experimental and analytical investigations to address fusing bearings and associated global

[1]Assistant Professor, Dept. of Civil Engineering, Univ. of Nebraska–Lincoln, Lincoln, NE 68583; formerly, Graduate Research Assistant, Dept. of Civil and Environmental Engineering, Univ. of Illinois at Urbana–Champaign, Urbana, IL 61801. E-mail: jsteelm2@illinois.edu; joshua.steelman@unl.edu

[2]Graduate Research Assistant, Dept. of Civil and Environmental Engineering, Univ. of Illinois at Urbana–Champaign, Urbana, IL 61801. E-mail: filipov1@illinois.edu

Note. This manuscript was submitted on September 5, 2012; approved on July 25, 2013; published online on July 27, 2013. Discussion period open until June 15, 2014; separate discussions must be submitted for individual papers. This paper is part of the ***Journal of Bridge Engineering***, © ASCE, ISSN 1084-0702/A4014007(14)/$25.00.

[3]Associate Professor, Dept. of Civil and Environmental Engineering, Univ. of Illinois at Urbana–Champaign, Urbana, IL 61801 (corresponding author). E-mail: fhnstck@illinois.edu

[4]Bridge Engineer, Parsons Corporation, 10 South Riverside, Ste. 400, Chicago, IL 60606; formerly, Graduate Research Assistant, Dept. of Civil and Environmental Engineering, Univ. of Illinois at Urbana–Champaign, Urbana, IL 61801. E-mail: revell2@illinois.edu; jessica.revell@parsons.com

[5]Professor, Dept. of Civil and Environmental Engineering, Univ. of Illinois at Urbana–Champaign, Urbana, IL 61801. E-mail: jlafave@illinois.edu

[6]Professor and Chair, Dept. of Civil and Environmental Engineering, Northeastern Univ., Boston, MA 02115. E-mail: jf.hajjar@neu.edu

[7]Professor Emeritus, Dept. of Civil and Environmental Engineering, Univ. of Illinois at Urbana–Champaign, Urbana, IL 61801. E-mail: dfoutch@illinois.edu

bridge response is sparse, although there is interest in using such structural elements as part of the seismic design methodology for certain regions of the United States. In particular, the Illinois DOT (IDOT) has developed an earthquake resisting system (ERS) (Tobias et al. 2008) that seeks to achieve acceptable seismic bridge performance by proportioning common bearing systems such that they experience predictable damage, act as force-limiting fuses between the superstructure and substructure, and allow the superstructure to slide on the substructure. This approach has been named quasi-isolated design because the system response resembles that of a conventionally isolated system (AASHTO 2010a) after bearings have achieved a fused state in that the superstructure can move relative to the substructure with minimal restraint. Although the configuration and design approach of a quasi-isolated system is significantly simplified relative to a conventionally isolated system, these benefits must be considered along with some limitations. Compared with a conventionally isolated system, there is larger uncertainty in the seismic response of a quasi-isolated one, and greater damage is expected, primarily at the bearings. However, compared with a conventional nonisolated system, a quasi-isolated system is expected to sustain less damage at the substructures. For a quasi-isolated bridge, support surface areas at substructures may need to be enlarged to prevent unseating at the bearings, and the bridge superstructure could be permanently offset following sliding of the bearings during a very large seismic event.

This paper presents results of a project conducted to experimentally investigate the behavioral characteristics of bearings and computationally assess the implications for global bridge response during seismic events when bridges are designed and constructed according to a quasi-isolation paradigm. The scope of the research project encompasses full-scale experiments of bridge bearings used in Illinois, together with nonlinear finite-element models of complete bridge systems (using numerical models of bridge bearings validated against the test results). Parametric studies have been conducted to explore system level seismic response for a range of representative Illinois bridges and to develop recommendations for seismic design of bridges using the quasi-isolation philosophy. The suite of bridges comprises combinations of continuous steel and concrete girder superstructures (each with relatively short and long span lengths options), wall and pier substructures (each with short and tall height options), and flexible and rigid foundations. Additional information may be found in Filipov (2012) and LaFave et al. (2013b). The basic prototype bridge considered in the parametric study is shown in Fig. 1. The key components to provide a quasi-isolated response are the bearings, which are elastomeric bearings at all substructures except for low-profile steel fixed bearings used at one of the piers. Typical details of the elastomeric bearings considered for the study are shown in Figs. 2(a and b) for bearings composed of a steel-reinforced elastomer block vulcanized to a thick top plate (IDOT Type I bearings), and in Fig. 2(c) for bearings that also include a flat polytetrafluoroethylene (PTFE) layer-on-stainless steel sliding layer (IDOT Type II bearings). A typical fixed bearing is shown in Fig. 2(d).

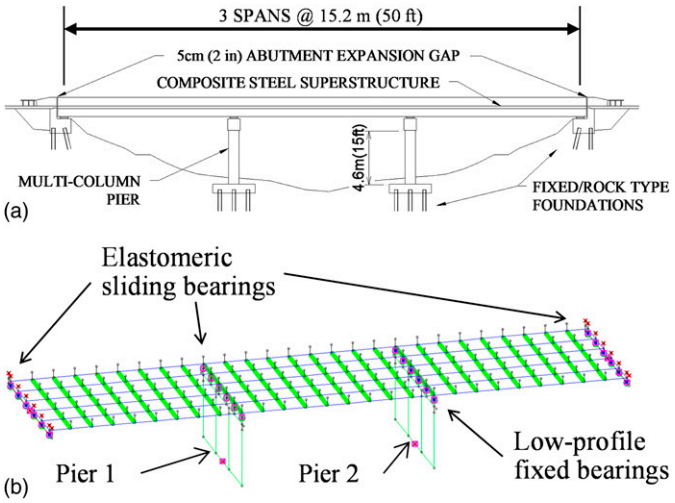

Fig. 1. Representative prototype bridge: (a) elevation view of base bridge; (b) global finite-element model

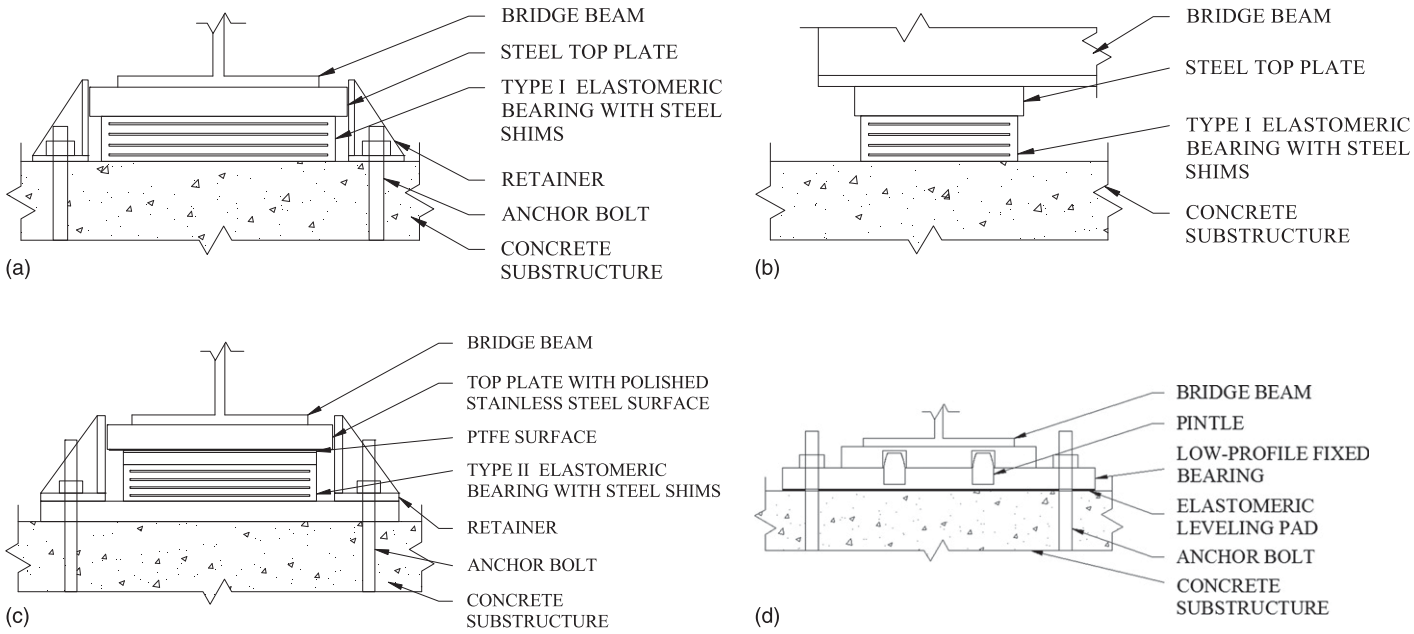

Fig. 2. Bearing types: (a) Type I, longitudinal view; (b) Type I, transverse view; (c) Type II, longitudinal view; (d) low-profile fixed, longitudinal view

A well-proportioned quasi-isolated bridge system will dissipate seismic energy through fusing and then sliding friction at the bearings, rather than via large inelastic structural demands in the substructures. Data from global bridge analyses (Filipov 2012; Filipov et al. 2013a, b) indicate that, for bridges with Type I elastomeric bearings and designed according to preliminary IDOT ERS guidelines (IDOT 2009), the piers of the prototype bridge are likely to have higher capacity than the bearing shear restraint elements when seismic demands are oriented principally in the transverse direction of the bridge. That is, transverse motion is likely to initiate damage at the concrete anchors providing restraint to the bearings (at the bottom plate of the fixed bearings or the side retainers at elastomeric bearings), and the bearings will then slide on pier caps and abutments after the anchors have ruptured. Piers may experience flexural cracking but are unlikely to exhibit inelastic response. In the longitudinal bridge direction, however, the elastomeric bearings exhibit a low shear stiffness and are unrestrained against motion in the longitudinal direction, except by friction. Therefore, the elastomeric bearings easily transition to the desired quasi-isolated response, and their supporting substructures are protected from large seismic force demands. The relatively high stiffness and force capacity of the fixed bearings attracts a disproportionate seismic demand, primarily resisted by large plastic response in the supporting pier. As the inelastic response at the fixed bearing pier increases, the abutment backfill provides a secondary energy sink. Localized damage to the abutment backwalls and backfill and the approach pavement have been deemed acceptable by IDOT, and so the primary impediment to the desired quasi-isolated response is the overstrength of the fixed bearings relative to the pier.

The experimental data presented in this paper focus on behavior observed from fixed bearing tests. Previous testing reported in the literature for fixed bearings is limited. The set of tests having the closest resemblance to the experiments reported herein were those described by Mander et al. (1996). They evaluated various types of fixed bearings retrieved from existing structures. Low-profile fixed bearings, nearly identical to those of the research described in this paper, were among those studied by Mander et al. (1996), but their testing apparatus was significantly different: the bearing specimens were mounted to steel assemblies designed to constrain the failure mechanisms to the pintles. Mander et al. (1996) did perform a subset of experiments with anchorage to concrete rather than a steel frame, but in those tests, the steel bearings were high (tall) fixed bearings, rather than low profile, and the concrete provided for support was a pedestal (rather than a large surface on which the bearing could slide). Consequently, behavior of those bearings on concrete from Mander et al. (1996) included rotational aspects of the bearing itself (high versus low), in addition to flexibility at the connection to concrete (flexural versus shear) and flexural response of the RC pedestal, but no sliding. The bearings, boundary conditions, and resulting limit states examined in the tests reported in this paper have been designed and constructed to simulate field conditions, in particular with regard to ultimate performance of anchors installed in concrete and subsequent sliding on concrete substructures.

Experimental Investigation of Low-Profile Fixed Bearings

Experimental Program Overview

The low-profile steel fixed bearing tests described in this paper are part of an extensive bearing experimental program that also included Type I and Type II elastomeric bearings (LaFave et al. 2013a). Tests were conducted to investigate the response of each type of bearing in both longitudinal and transverse orientations. The tests were performed in the Newmark Structural Engineering Laboratory at the University of Illinois, using a customized experimental apparatus described in detail in Steelman et al. (2013). The bearing test apparatus (Fig. 3) consisted of a pair of vertical actuators and a horizontal actuator attached to a loading beam, so that a prescribed gravity loading could be maintained while at the same time simulating large horizontal displacements. Concrete pads were cast (Fig. 4) and attached to the strong floor to represent typical bridge substructures, including a brushed top finish as specified by IDOT (IDOT 2007) to ensure that any frictional response at the substructure interface appropriately reflected expected field conditions.

A total of two test pads were used for the fixed bearing tests, one each for the two weak anchor designs and the two weak pintle designs. Each pad measured 2.13×1.22 m (7×4 ft) in plan and had a thickness of 406 mm (16 in.). Reinforcing grids were placed at the top and bottom of each pad, as shown in Fig. 4 (including dimensions indicating the approximate distances from centers of anchors to the edges of bars at the top surface). The inset image in Fig. 3 shows a detailed view of the weak anchor specimen oriented to simulate longitudinal bridge motion, where motion is imposed on the bearing in the x-direction indicated in the figure. After that test was completed, a new bearing (also designed to fuse at anchors) was installed with a footprint rotated 90° on the concrete surface of the same concrete pad to simulate transverse bridge motion. This sequence was selected to minimize the interference of the failure zones at anchors from a previous test on a subsequent test. After completing both the longitudinal and transverse simulations with weak anchor designs, the concrete pad [Fig. 4(a)] was removed and replaced with an identical pad [Fig. 4(b)], and the tests were repeated with weak pintle fixed bearing designs.

Fixed Bearing Specimen Designs

The bearings were designed using AASHTO M270M Grade 250 (M270 Grade 36) steel for a typical Illinois highway bridge [Fig. 1(a)] in accordance with the *IDOT Bridge Manual* (IDOT 2009) and IDOT standard specifications for road and bridge construction (IDOT 2007), resulting in the dimensions shown in Figs. 5–7 (all dimensions shown are in millimeters). The total design vertical load for a bearing was 299 kN (67.2 kips). Two design options were considered: weak anchors and weak pintles. Plate widths in the longitudinal bridge direction, plate thicknesses, and pintle sizes were the same for both cases. Pintles at fixed bearings are steel cylinders, typically 32 mm (1.25 in.) in diameter, press-fit into the bottom plate to a depth of 25 mm (1 in.); the upper 22 mm (7/8 in.) of each pintle is tapered with a radius of 76 mm (3 in.). The pintles used for the test specimens conformed to these typical dimensions. Also in accordance with standard details used by IDOT, the pintle holes in the upper plate were oversized by 3 mm (1/8 in.) in diameter, and the bottom surface of the top plate was rounded to a radius of 610 mm (24 in.). These fabrication details, in conjunction with the tapered upper portions of the pintles, permit these bearings to tolerate small flexural rotations of bridge girders without inducing significant moment demands on the connection of the bearing to the substructure.

For the weak anchors option, the minimum anchor size and grade used by IDOT were specified; i.e., 19 mm (3/4 in.) diameter and ASTM F1554 (ASTM 2007) Grade 36 (248-MPa yield strength). For the weak pintles option, the shear strength of the anchors was increased with the intention of generating ruptures in pintle(s) prior to the anchors reaching their ultimate strength. Consequently, although the pintles remained at the minimum size used by the IDOT, anchor diameters were increased from 19 (3/4 in.) to 38 mm (1.5 in.), and the specified material strength of the anchors was ASTM F1554 (ASTM 2007) Grade 105 (724-MPa yield strength).

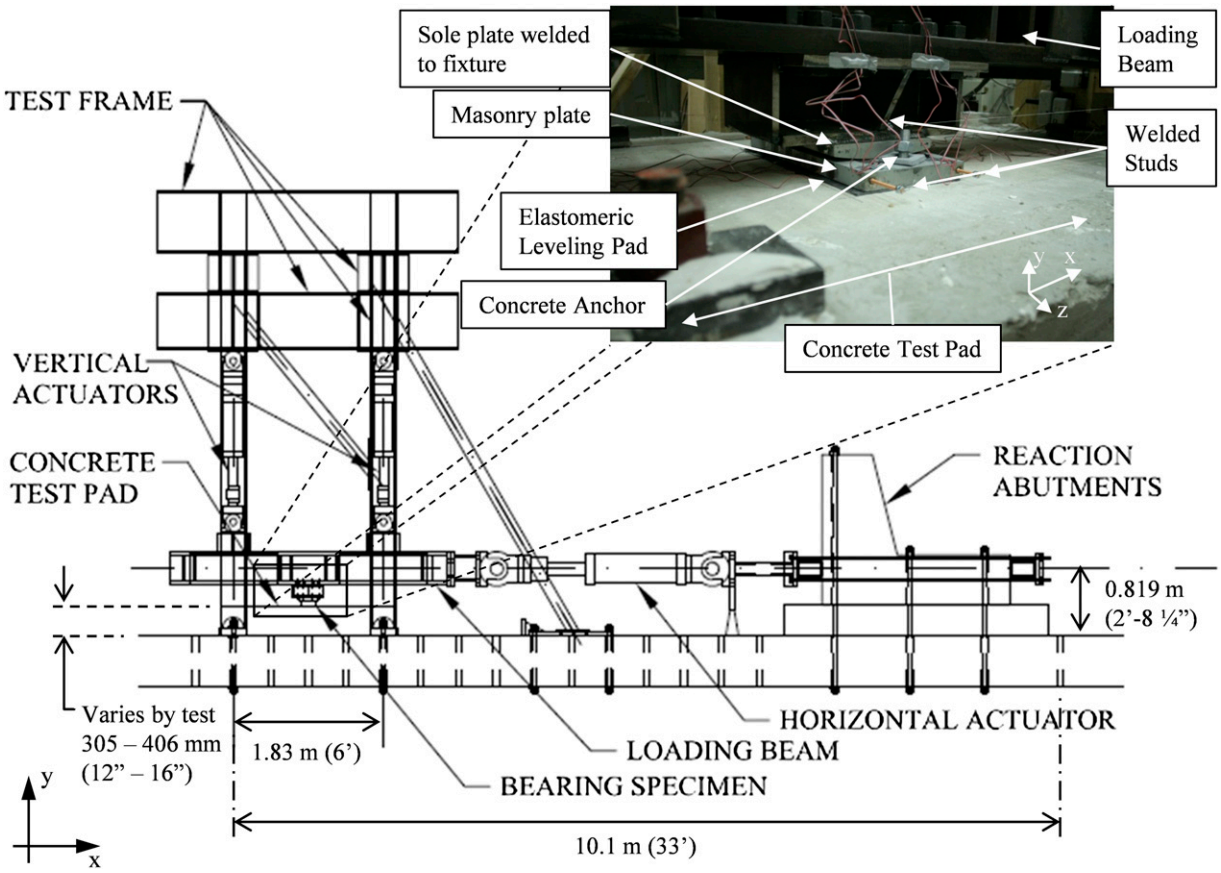

Fig. 3. Test frame elevation

In all fixed bearing cases, the top plate was welded all around to the bottom of a built-up steel fixture mounted to the underside of the loading beam. The bottom of the steel fixture was sized to simulate the bottom flange of a typical steel girder, with a plate thickness and width of 19 mm (3/4 in.) and 254 mm (10 in.), respectively. The width of the simulated girder flange was the primary characteristic that determined the width of the sole (top) plate in the transverse direction of the bridge, whereas the masonry (bottom) plate was sized to provide adequate clearance for the anchors.

Estimated Fuse Capacity

The estimated fuse force was calculated based only on the anticipated ultimate pure shear capacity of the anchors or pintles, in accordance with IDOT standard practice (IDOT 2009), as

$$V_{\text{fuse}} = \phi n 0.6 F_u A_b \tag{1}$$

where ϕ = strength reduction factor (taken as unity, to reflect nominal capacity); n = number of shear transfer elements; the 0.6 coefficient reflects the assumption that pure shear controls capacity; F_u = ultimate tensile strength of the material under consideration; and A_b = effective cross-sectional area of a single shear transfer element. The value of n is 2 for either bolts or pintles. The effective area was calculated as 80% of the nominal cross-sectional area for the threaded anchors into concrete [consistent with AASHTO Section 6.13.2.12 and the commentary for 6.13.2.7 (AASHTO 2010b)], whereas the full area was used for pintles. Calculations for each potential fuse element for both options are summarized in Table 1.

Rupture capacities are provided for fusing components in each design case in Table 1. Yield capacities are also included to illustrate that large deformations were anticipated to be constrained to the selected fusing shear planes in each design case. Uniaxial tension yield strengths, F_y, and ultimate strengths, F_u, are provided, as appropriate to the limit state noted for each combination of component and design case. Yield and ultimate strengths shown in the table for anchor elements used for both weak anchor bearing designs [ASTM F1554, Grade 36 (ASTM 2007)] and weak pintle bearing designs [ASTM F1554, Grade 105 (ASTM 2007)] were obtained from coupon tests of the anchor material. Samples of the steel used for pintles could not be obtained from the bearing manufacturers, so mill reports were the only source of material information available. In the case of the weak anchor designs, even the minimum steel strength [248 MPa (36 ksi)] provides a significant margin between the yield strength of the pintles and the anticipated ultimate fuse capacity of the anchors. The coupon tests for the anchors used for the weak anchor fixed bearings indicated that the yield and ultimate tensile strengths were approximately 345 (50 ksi) and 505 MPa (73 ksi), respectively. Accounting for the relatively high anchor material strength, the anchors were still expected to control the weak anchors test fuse capacity, at about 59% of the lower bound of the minimum pintle yield capacity.

Documentation supplied by the bearing manufacturer for the pintle design cases indicated that, although M270/Grade 36 (A709) material had been used for the sole and masonry plates, the material used for the pintles was M222 (A588), with an average ultimate tensile strength of 563 MPa (81.6 ksi) according to the mill report. This average value from the mill report was used when calculating

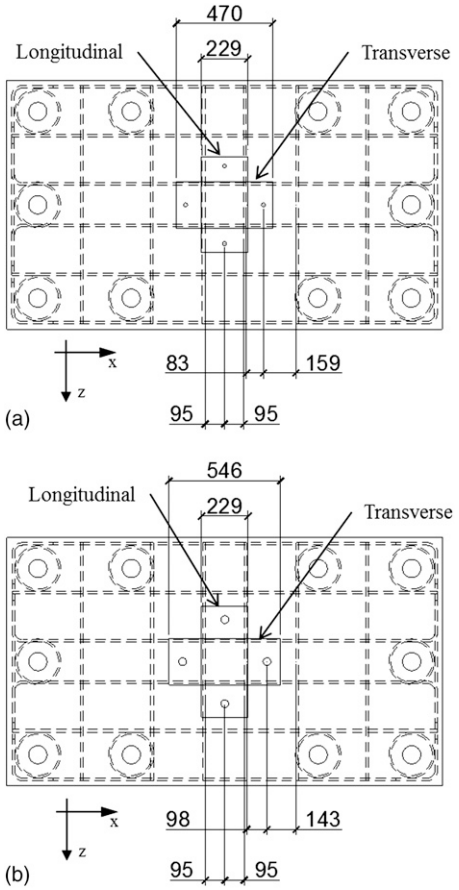

Fig. 4. Concrete pad reinforcing layout and approximate anchor locations relative to bars (in mm): (a) weak anchors; (b) weak pintles

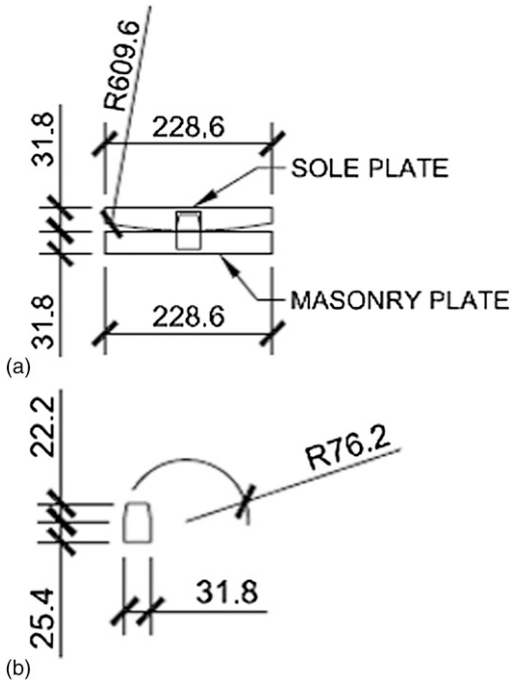

Fig. 5. Fixed bearing section cut parallel to bridge longitudinal axis and pintle detail (in mm): (a) longitudinal section; (b) pintle detail

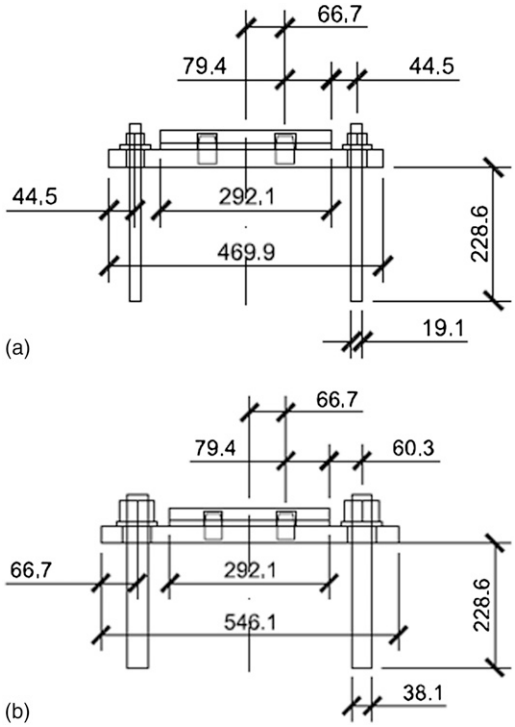

Fig. 6. Fixed bearing section cuts parallel to bridge transverse axis (in mm): (a) weak anchors; (b) weak pintles

the estimated fuse capacity for the pintles in the weak pintle tests. Coupons matching the anchors supplied for the weak pintle tests were tested and exhibited yield and ultimate tensile strengths of approximately 827 (120 ksi) and 989 MPa (143.5 ksi), meeting the specified material grade requirements. Consequently, using the mill report data for the pintles and the coupon test data for the anchors, the estimated fuse capacity based on pintle shear strength was 534 kN (121 kips) or about 59% of the estimate for pure shear yielding of the anchors for the weak pintles case.

Testing Protocol

Two specimens were tested for each design case (weak anchors versus weak pintles), for a total of four tests. For each design case, separate tests were conducted to investigate the response of the bearings when subjected to longitudinal versus transverse bridge movement. In addition to the position and force measurements recorded from the actuators, cable extension transducers (CETs) were attached to the specimens at six locations. A pair of welded studs was mounted to opposite sides of the steel fixture (to which the sole plate was welded), and one welded stud was mounted to each corner of the masonry plate, as shown in the inset image of Fig. 3. The CETs provided measurements for relative translations of the sole plate with respect to the masonry plate and also plan rotations of the masonry plate on the concrete surface. All fixed bearing tests were carried out with a target simulated gravity load of 187 kN (42 kips). The previously indicated design load was intended to represent the maximum total load that would be imposed on the bearing, and therefore it was reduced for these experiments to reflect the fact that full live load is not expected to be imposed during a major seismic event.

The testing protocol for the low-profile fixed bearings started with a set of force-based cycles, which then transitioned to displacement-based cycles for postfusing sliding behavior. The force-based cycles

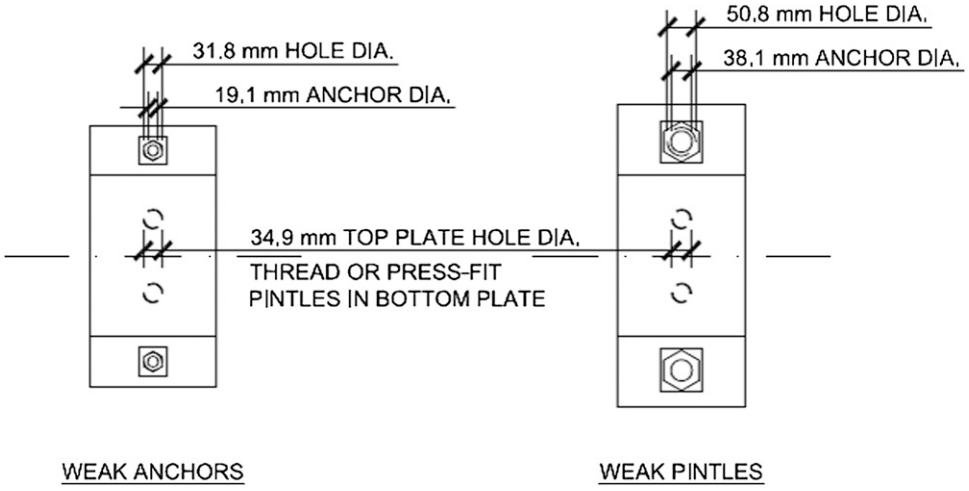

Fig. 7. Fixed bearing plan views

Table 1. Estimated Fuse Capacities

	Fuse design case			
	Weak anchors		Weak pintles	
Parameter	Anchors	Pintles	Anchors	Pintles
ϕ	1			
n (elements)	2			
Diameter (mm)	19	32	38	32
Thread adjustment	0.8	1	0.8	1
A_b (mm^2)	228	792	912	792
Limit state	Rupture	Yield	Yield	Rupture
F_y or F_u (MPa)	505	248	827	563
V_{fuse}, estimated (kN)	138	236	906	534

included three sets of three cycles each at 25, 50, and 70% of the estimated fuse force capacity of the bearing. After completing these initial nine force-based cycles, the testing protocol transitioned to displacement-based targets. Benchmark targets equal to 25, 50, 100, 200, 300, and 400% of 48 mm (1-7/8 in.), corresponding to displacement targets used in companion elastomeric bearing tests, were imposed in sets of three cycles each. Additional intermediate cycles were inserted to transition between the early benchmark thresholds, with incremental increases of 5% or 2.5 mm (0.1 in.) per cycle prior to the realization of a fully fused shear plane with pure sliding behavior. The longitudinal weak pintles test was a special case, where the additional cycles were foregone for cycles to displacements larger than 48 mm (1-7/8 in.), and the test ended with only two cycles to the 300% target, one cycle to 400%, and a final monotonic excursion to create a fully fused state at the pintles.

Tests were conducted at quasi-static rates, with small incremental position adjustments progressing through the force and displacement protocol, as well as to correct the vertical load when out of tolerance. Initial cycle targets were established at force levels proportionate to the estimated fuse capacity of a bearing, but all actuators were controlled with position feedback throughout testing. Resultant horizontal forces were used to determine step target convergence in the initial cycles, but the substeps taken to reach each step target were incremental and displacement-based (i.e., substep displacement targets were incrementally increased until the step force target was reached). The test durations were influenced by data sampling and calculations for control of the three actuators, periodically requiring adjustments to the vertical actuators to maintain the simulated gravity load within a tolerance, and therefore the total time required to conduct a single test ranged from about 8 to 16 h. Vertical loads were adjusted when the resultant vertical reaction from the actuators deviated from the target load of 187 kN (42 kips) by a specified amount, ranging from 11 to 20 kN (2.5–4.5 kips). Horizontal displacements were imposed on the bearings in substep increments of 0.32 mm (0.013 in.) during the force-based cycles and 0.48 mm (0.019 in.) increments for the displacement-based cycles.

Experimental Results

Constitutive Force-Displacement Response

The general response for the weak anchor tests shown in Figs. 8 and 9 is consistent with expectations based on fundamental mechanics considerations and corroborated in Mander et al. (1996). In both orientations, the response is a combination of sliding friction and mechanical shear resistance provided by the anchors. Observations of the anchor rupture surfaces following the tests showed that the fractures were planar pure shear failures at the top of the concrete surface. A stable hysteretic response was also obtained in each orientation for large sliding displacements.

The constitutive response for the weak pintle designs is shown in Figs. 10 and 11, and the mechanical characteristics observed for the weak pintle cases were significantly more complicated than for the weak anchor cases, with neither orientation exhibiting the intended ultimate behavior: fractured pintles and intact concrete anchors. The response for both orientations was influenced by local concrete failures, as seen at the concrete pad surface after completion of both weak pintle tests and removal of the pad from the test frame (Fig. 12). Additionally, the more complex progressive failure sequence for the longitudinal orientation is shown in Fig. 13. A plan view of the masonry plate is provided in the lower right corner of each frame to indicate which elements have ruptured at each stage (solid circles), with the outer circles representing the concrete anchors and the inner circles representing the pintles.

In the early stages of the longitudinal orientation test, with all elements intact, the masonry plate appeared to rotate about an axis parallel to the long direction of the bearing (a rollover response in the longitudinal direction of the bridge). This rotation was accommodated by the curved bottom surface of the sole plate [Fig. 5(a)], the rounded top sections of the pintles [Fig. 5(b)], minor crushing of

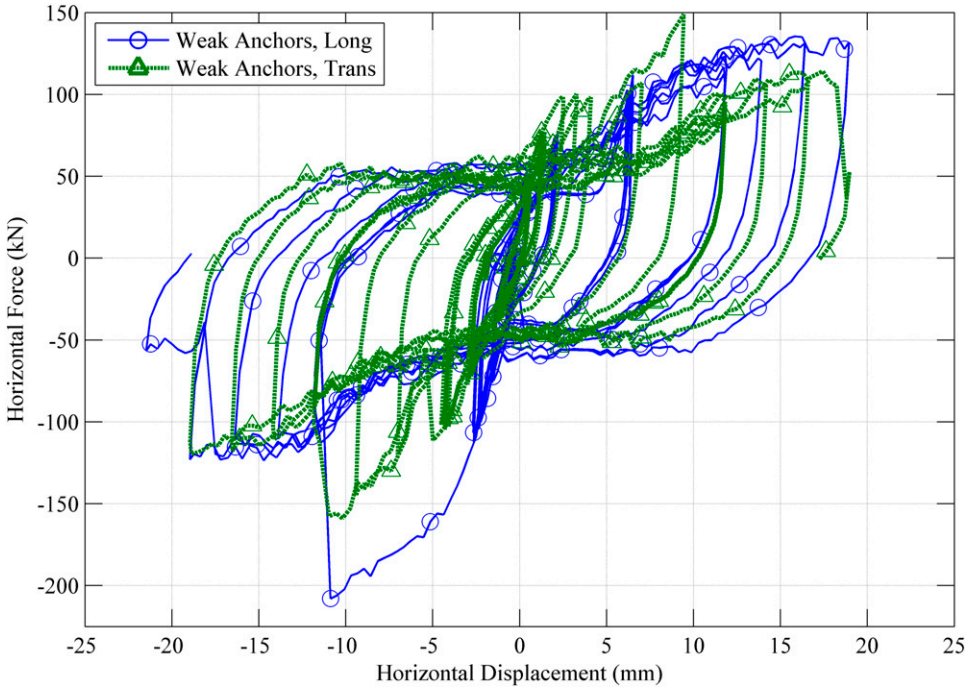

Fig. 8. Force versus displacement response to fully fused state for weak anchor tests

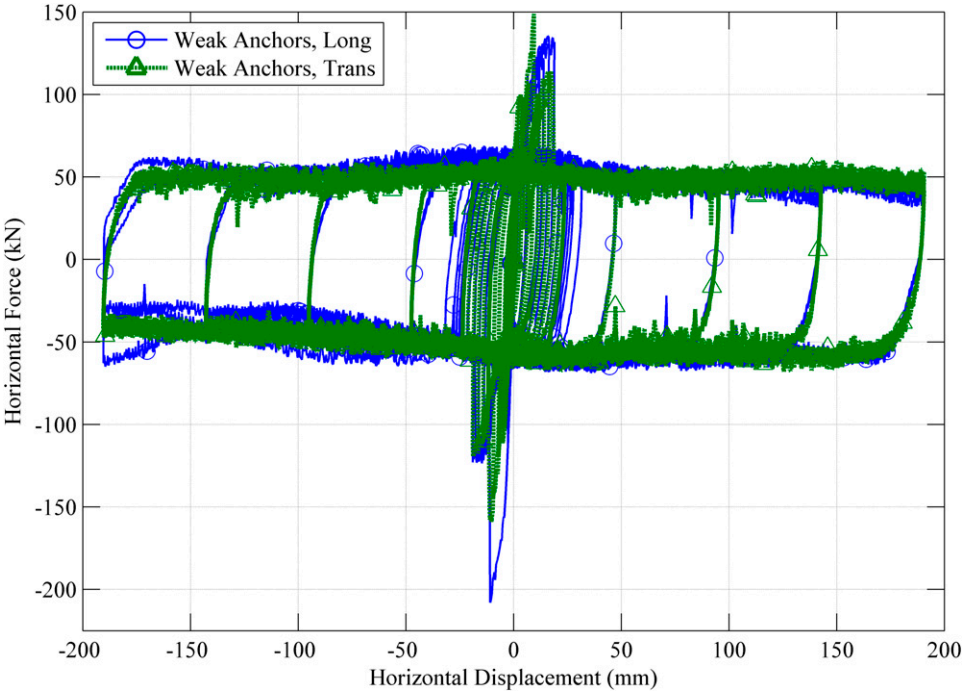

Fig. 9. Force versus displacement response for complete weak anchor tests

concrete at the leading edge of the masonry plate, and a slight raising of the sole plate to maintain the target vertical load (when the induced vertical compression exceeded the tolerance). This mechanism induced complex flexural and tensile demands in the anchors in addition to the anticipated shear. Meanwhile, the rounded tops of the pintles, oversized holes in the sole plate, and curved bottom surface of the sole plate permitted the relative rotation of the sole and masonry plates without inducing significant demands in the pintles. Consequently, the peak force capacity was determined by the anchors, rather than the pintles, and the first rupture occurred at a loading beam (i.e., superstructure) displacement of about −40 mm (−1.6 in.). The anchor rupture occurred about 45 mm (1.75 in.) below the concrete surface as noted in Fig. 12. Following the failure of one of the anchors, the masonry plate pivoted about the remaining anchor, whereas the sole plate was restrained from rotating by the loading beam, causing the pintles to resist a couple in

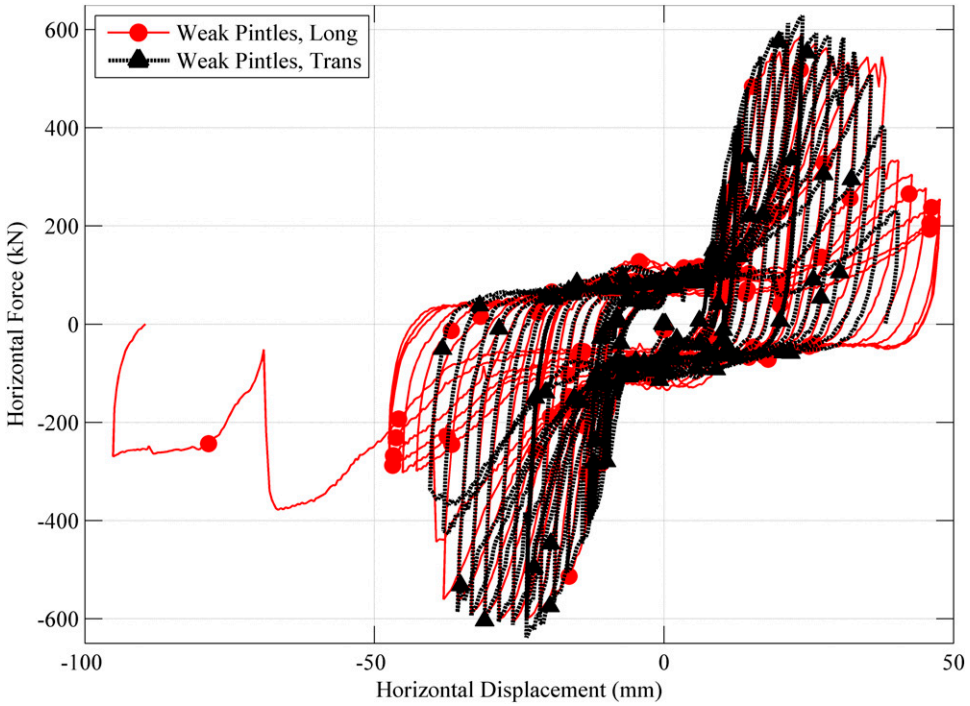

Fig. 10. Force versus displacement response to fully fused state for weak pintle tests

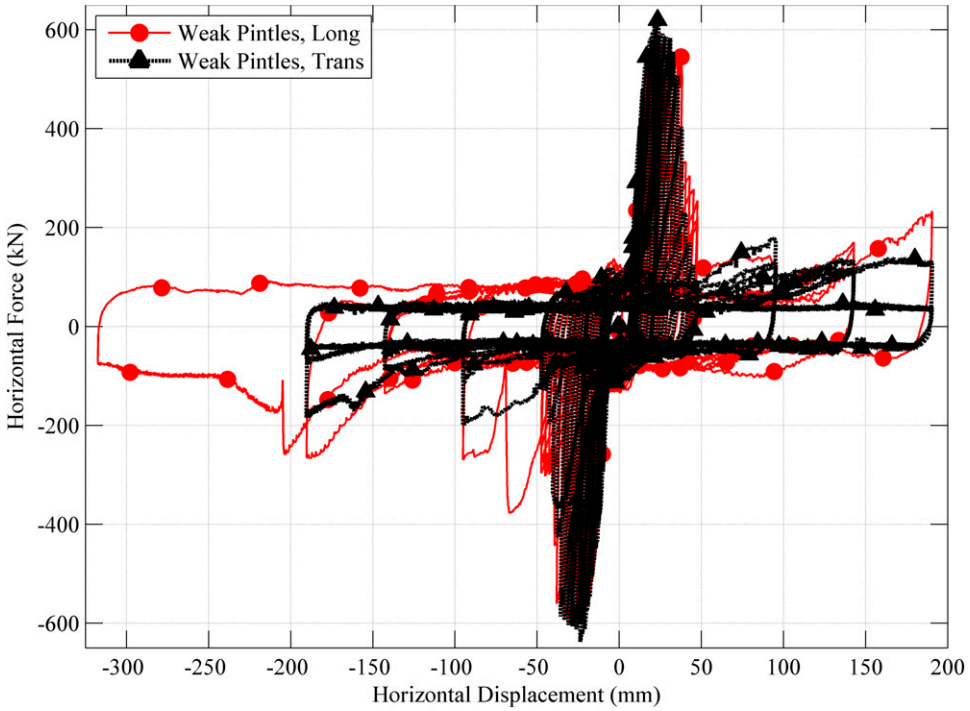

Fig. 11. Force versus displacement response for complete weak pintle tests

addition to direct shear. Because of these mechanical demands, the pintle nearer to the remaining anchor failed at a displacement of about −70 mm (−2.75 in.). With only one anchor and one pintle remaining, the rotation of the masonry plate became more pronounced, and the cyclic protocol was foregone in favor of a monotonic ramp to fail the remaining pintle, which finally occurred at approximately −200 mm (−7.8 in.).

In the transverse weak pintles case, both of the anchors failed, and the pintles remained intact, although plastically deformed. It appeared that the concrete crushed locally around the high strength anchors and that the extent of the concrete damage extended outward from the anchors and downward with succeeding cycles. The rupture surfaces of the anchors were approximately 50–65 mm (2–2.5 in.) below the surface of the concrete pad, and

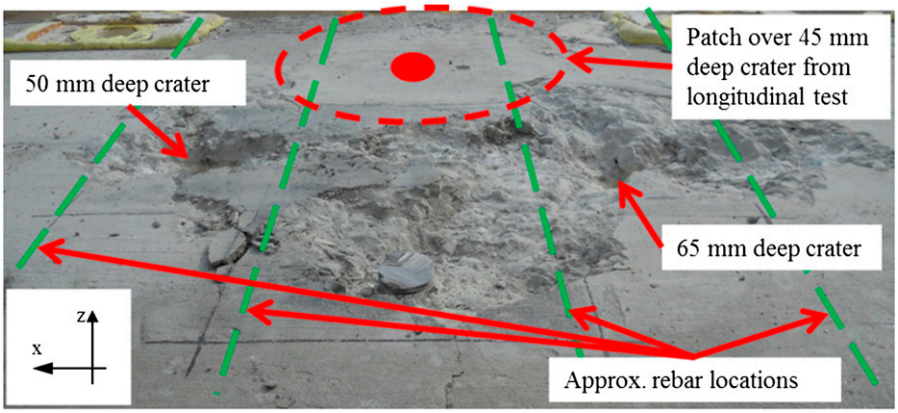

Fig. 12. Concrete surface condition after completion of weak pintle tests

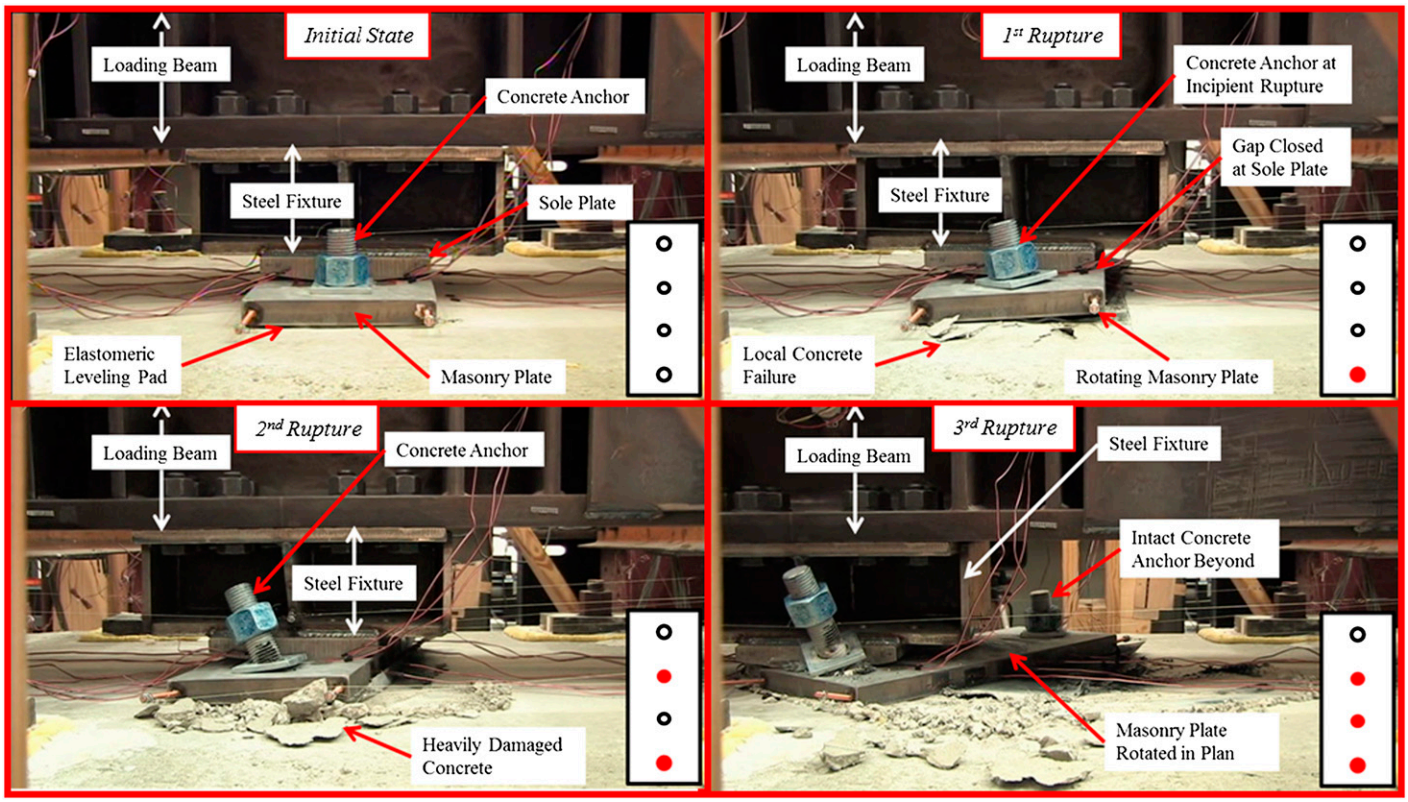

Fig. 13. Failure stages during longitudinal weak pintles test

rupture occurred at bearing displacements of approximately 40 mm (1.5 in.) in each direction in Fig. 10. The crushed concrete led to mechanical demands on the anchors similar to driven piles in soil, with a combination of shear and flexure. After the anchors had failed, they continued to influence the response, as seen in Fig. 11, where each new displacement level exhibited a clear increase in shear resistance above typical sliding resistance as the remnants of the anchors that extended below the masonry plate were dragged through undamaged concrete. Both weak pintle specimen failures were precipitated by anchor failures, rather than pintle failures, so the mill report data for the pintles were only used to define the loading protocol. Coupon test results for the pintles were not necessary to characterize the failure mechanism for these designs.

Sliding Response

Eq. (1), which was used to estimate fuse force capacity for the purposes of specifying a loading protocol, does not include a term to account for friction response, but Figs. 8–11 show that friction is not negligible in the total response, especially for the weak anchor bolt cases. Average values of sliding force and corresponding apparent friction coefficient, μ, when normalized by the instantaneous vertical load [approximately 187 kN (42 kips)] are shown in Table 2 for the individual tests. The postfusing response is partitioned from the full test results to isolate the sliding resistance in the absence of anchor or pintle element influences.

Displacements were primarily accommodated by sliding at the steel-elastomer interface, although slip also occurred at the steel plate interface, and the sliding response was further complicated by

crushing of concrete near the anchors for the weak pintle cases. In the transverse orientation for weak pintles, in particular, the thin elastomeric pad was torn and ground into multiple pieces as the fractured anchor remnants were dragged through the concrete. Considering the dependency of the weak pintle test results on various mechanisms causing concrete damage, the values obtained for the weak pintle cases should be considered less reliable than the values for the weak anchor tests.

Fuse Force Capacity

Calculations to compare observed and nominal force capacities, accounting for the influence of friction, are provided in Table 3. Peak force is the maximum absolute value of shear resistance obtained during each individual test. This force is reduced by the postfusing sliding resistance values shown in Table 2 and compared with the estimated nominal capacity obtained from Eq. (1) to obtain the percent difference of the observed resistance relative to the nominal resistance.

The observed capacity inferred for the longitudinal weak anchor test generally possessed higher strength than estimated based on the assumptions implicit in Eq. (1) and material strength obtained from ancillary tests of anchor material. The difference is likely a result of uncertainty in actual material strength of the anchors for the test specimen and a stress state that incorporates minor tension components from deformations at incipient anchor rupture. In contrast, the transverse weak anchor test exhibited a capacity inferred to be about 22% less than the nominal capacity at mean postfusing sliding resistance. The likely cause of the difference between the longitudinal and transverse tests lies with the installation procedure. The anchors were drilled and epoxied into the concrete pad using HILTI HY-150 (Hilti Corporation, Schaan, Liechtenstein) injected epoxy with the masonry plate in place. In both tests, one of the anchors was inadvertently installed with an excess of epoxy, resulting in epoxy being pushed upward to fill the space between the anchor and the hole in the masonry plate. For the longitudinal test, there was sufficient space around the other bolt and the pintles so that the bottom plate could rotate slightly in plan and engage both anchors. For the transverse test, the anchor with excess epoxy had to carry the full shear load (in excess of friction) until deforming sufficiently to close the gap at the other bolt hole. Thus, one of the bolts was carrying a disproportionate share of the total shear when the peak capacity was achieved for the bearing, and the full strength of the other bolt was not realized, resulting in an observed capacity noticeably less than the estimated nominal strength.

The strengths for the weak pintle cases are surprisingly close to the nominal value, but considering that neither orientation exhibited the intended mechanism corresponding to the estimated nominal strength, this outcome must be considered coincidental. The experiments demonstrate that unanticipated mechanisms can influence the performance of pintle-controlled designs, potentially resulting in

Table 2. Observed Sliding Resistance

		Fuse case			
		Weak anchors		Weak pintles	
Data inclusion range	Sliding parameter	Longitudinal orientation	Transverse orientation	Longitudinal orientation	Transverse orientation
Full test	Coefficient of friction, μ				
	Minimum	0.13	0.11	0.13	0.07
	Mean	0.28	0.27	0.37	0.26
	Maximum	0.41	0.40	0.66	0.74
Postfusing only	Sliding force (kN)				
	Minimum	24.4	20.5	24.8	13.3
	Mean	52.9	51.0	70.8	43.1
	Maximum	69.6	67.9	103.2	96.1
	Coefficient of friction, μ				
	Minimum	0.13	0.11	0.13	0.07
	Mean	0.28	0.27	0.37	0.23
	Maximum	0.37	0.35	0.54	0.53

Table 3. Comparison of Nominal and Observed Capacity

	Fuse case			
	Weak anchors		Weak pintles	
Quantity	Longitudinal orientation	Transverse orientation	Longitudinal orientation	Transverse orientation
Peak force (kN)	208	159	606	637
Anchor capacity (kN)				
Maximum	183	138	581	624
Mean	155	108	535	594
Minimum	138	91	503	541
V_{fuse}, estimated (kN)	138	138	534	534
Percent difference @ (percentage)				
Maximum	33	0	9	17
Mean	12	−22	0	11
Minimum	0	−34	−6	1

greater damage to substructures than would have been observed for anchor bolt–controlled designs. Although it may be possible to proportion a fixed bearing to achieve reliable fusing response from pintle fracture, the results from this experimental program indicate that anchor bolt fracture is the more reliable and predictable fusing mechanism. Even if a long bridge span was to be supported by fixed bearings designed to fuse at pintles, or if the minimum pintle size is permitted to be reduced in the future, a pintle-controlled design is still not likely to be preferable to an anchor bolt–controlled design. The postfusing response of a pintle-controlled design will be more complex than an anchor bolt–controlled design, with potential interactions between the sole plate and upper portions of anchors extending into nuts above the masonry plate (in the transverse direction) or unseating from the masonry plate in the longitudinal direction, followed by an even higher peak load during a reversal in the unseated configuration.

Global Bridge Response

The central objective of the quasi-isolation design paradigm is that seismic damage can be primarily limited to the bearings as sacrificial elements (and abutment backwalls, if necessary), so that piers and foundations remain largely undamaged following a large seismic event. Global bridge models were necessary to investigate whether the anticipated bearing behavior and associated substructure response conforms to this premise, and particularly how the relative stiffness and anchorage of the fixed bearings influences the local pier and global bridge response, when considered in conjunction with elastomeric bearings at other substructure units. The global bridge model was also used to investigate the efficacy of selected modifications to design and construction practice, such as reducing the number of fixed bearings that are anchored to the substructure (thereby limiting the fuse force that can be transferred to the supporting pier).

Prototype Bridge and Modeling Overview

The prototype bridge (Fig. 1) was a three-span continuous steel I-girder superstructure on two multicolumn (4) pier substructures [all proportioned in accordance with the *IDOT Bridge Manual* (IDOT 2009)]. The bridge deck width used for the analysis allows for two lanes of traffic and was modeled with six W27 × 84 (AASHTO M270/ASTM A709 Grade 50) girders that act compositely with a 20.3-cm-thick (8-in.-thick) concrete deck. The modeled height for the multicolumn piers of the prototype bridge was 4.5 m (15 ft). As shown in Fig. 1(b), low-profile fixed bearings were modeled at the second intermediate pier (Pier 2), whereas IDOT Type I elastomeric expansion bearings were modeled at the other pier and abutment locations.

Global analysis of complete bridge response was performed using a three-dimensional model in *OpenSees* (McKenna et al. 2006), incorporating material and geometric nonlinearities in time history analyses with a suite of ground motion records. A brief overview is presented here, and additional details of modeling assumptions, formulations, and results can be found elsewhere (Filipov 2012; Filipov et al. 2013a, b; LaFave et al. 2013b). The superstructure was modeled with a grid of linear elastic elements to capture the vertical flexural stiffness of the composite beams and the horizontal in-plane rigidity of the deck. Pier caps and pile caps at piers and abutments were modeled with linear elastic elements, and foundations were modeled with fully fixed nodes. At each abutment, the end nodes of the superstructure were connected to a backwall element with a 5-cm (2-in.) gap model to represent a thermal expansion joint, as noted in Fig. 1(a). On closing the gap, the superstructure engages the abutment backwall and backfill. The backwall was modeled with an elastic-plastic flexural joint at the connection of the abutment pile cap and backwall, and the backfill was modeled with a hyperbolic gap material. The pier column bents were composed of a specified plastic hinge length at each end of the element, modeled with distributed plasticity fiber sections, and a linear elastic component at the center of the element.

Type I elastomeric bearings were modeled with coupled bidirectional friction stick-slip response to seismic demands induced in the longitudinal and transverse directions of the bridge. The bearings were modeled with a static initial coefficient of friction of $\mu_{SI} = 0.45$, a kinetic coefficient of friction of $\mu_K = 0.30$, and a post-slip coefficient of static friction of $\mu_{SP} = 0.35$. The elastic stiffness of the elastomeric bearings was calculated as the shear modulus of the elastomer times the plan area of the bearing divided by the total height of rubber (not including reinforcing shims). A shear modulus of 585 kPa (85 psi) was used based on previous experimental results (Steelman et al. 2013). The transverse direction also included a bilinear hardening model with a pinching response for cyclic loading and fracture at ultimate to represent the presence of retainers with a single anchor. The capacity of these retainer anchors was estimated based on a modified Eq. (1), where the factor of 0.6 has been neglected because these elements experience a complex failure mechanism that is not accurately characterized solely by the pure shear of the anchor. The retainer anchor diameter was modeled as 1.6 cm (0.625 in.) at the abutments and 2.5 cm (1 in.) at the intermediate pier. For all elements modeled, the nominal capacities and material properties were used [e.g., $F_u = 415$ MPa (60 ksi) for anchor bolts].

For the fixed bearings, a bidirectional element was developed to capture the coupled elastoplastic response of a typical fixed bearing, including a pinched cyclic response and ultimate fracture of the concrete anchors, accounting for the time-varying resultant direction of the seismic demand. Friction was modeled in the same fashion as the elastomeric bearings; however, the coefficients of friction were kept constant at $\mu_{SI} = \mu_{SP} = \mu_K = 0.30$. The fuse capacity was based on Eq. (1) with two 1.9-cm (0.75-in.) anchors, and the pintle response was neglected because those components remain elastic in this scenario. In some cases, fixed bearings were modeled as unanchored, indicating that friction was considered, but no contribution from the anchors was accounted for in the model. The computational modeling parameters for fixed bearings were validated using experimental data presented in the previous section (Fig. 14). Fusing was intended to occur at the top of the substructure for Type I and fixed bearings, corresponding to the fracture of concrete anchors followed by sliding at the elastomer-concrete interfaces for Type I bearings and at steel-elastomer interfaces for fixed bearings.

Variations of Global Parameters

General trends for the baseline prototype bridge subjected to a suite of synthetic records developed by Fernandez and Rix (2006) for Paducah, Kentucky, at a 975-year return interval are summarized, and then the response to an alternate bridge design case is compared with the baseline case for one record. In the transverse direction of the bridge, the piers responded in double curvature and exhibited higher capacity to resist seismic demands prior to yield compared with a single curvature response in the longitudinal direction. Fixed bearings and elastomeric bearings both exhibited initially stiff response prior to fusing, with each bearing type restrained by steel anchors into the concrete substructures. Induced seismic force demands transferred through the bearings were approximately proportionate to the tributary seismic mass at each substructure support when the bridge was subjected to transverse excitation. Consequently, the seismic behavior in the transverse direction was close to an optimal

quasi-isolated response, with fixed bearings and retainers fusing while the sub- and superstructures remained essentially elastic.

On the other hand, in the longitudinal direction the bridge was found to have significantly higher susceptibility to undesirable locations and severity of damage, which is inconsistent with the desired response of a quasi-isolated design. Two primary modeling characteristics emerged as critical to the performance of the bridge in the longitudinal direction: fixed bearing fuse capacity and abutment resistance. The fixed bearings had stiffness and force capacity far exceeding the shear stiffness and sliding resistance of rubber-on-concrete at Type I bearings or PTFE-on-steel at Type II bearings, and therefore are anticipated to attract disproportionate seismic demand and induce damage in the substructure beyond superficial cracking and spalling for large seismic events. For example, piers with fixed bearings had base shears 14% higher than those with sliding bearings, and most parametric variations of superstructure, substructure, and foundation characteristics resulted in the pier with fixed bearings yielding (Filipov et al. 2013a). The abutments were also significant influences on longitudinal response through absorption of seismic energy as plastic deformations of the backwalls and backfill. In large earthquakes, the backwall and backfill elements could experience up to three times as much lateral load as the quasi-isolation system, and longitudinal displacements could be limited to about a quarter of what it would be if no such elements are installed (Filipov et al. 2012).

To address the influence of the fixed bearings on longitudinal response, three new fixed bearing configurations are proposed, with the goal of providing the desired fusing behavior for the design level earthquake. This is achieved by using fewer bearings with positive constraint (anchor bolts) and simply allowing the other low-profile bearings to slide on the elastomeric leveling pads (unanchored bearings). The variations include six (i.e., all, as a baseline), four, two, and zero fixed bearings installed with anchorage to the substructure, and unanchored (friction only) bearings provided at the remaining bridge girder support points. Fig. 15 shows the cases with (a) six and (b) zero fixed bearings. When anchorage is removed in the model, it is done progressively from the bridge centerline outward toward the parapets (e.g., in the case with two anchored bearings, the interior four bearings nearest the bridge centerline are unanchored).

Fig. 15 shows the general observed pier and bearing behavior for two bridge cases under different longitudinal intensities of shaking with a sample ground motion record from the suite of synthetic records developed by Fernandez and Rix (2006) for Paducah, Kentucky, at a 975-year return interval. Details of the scaling procedure used to correlate the ground motion at Paducah to a spectrum consistent with USGS hazard maps adopted by AASHTO for seismic design at Cairo, Illinois, are available in Filipov et al. (2013a). This seismic hazard level at Cairo, Illinois, is treated as a baseline reference [scale factor (SF) = 1]. The individual piers are referred to in the figure as Pier 1 for the pier with elastomeric bearings and Pier 2 for the pier with fixed bearings. The first column of plots shows that for Pier 1, the elastomeric bearings are capable of accommodating displacement demands at the reference hazard level (SF = 1) by sliding and by

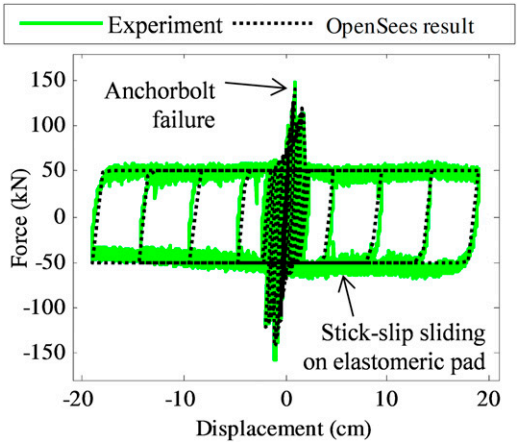

Fig. 14. Validation of computational model with experimental data

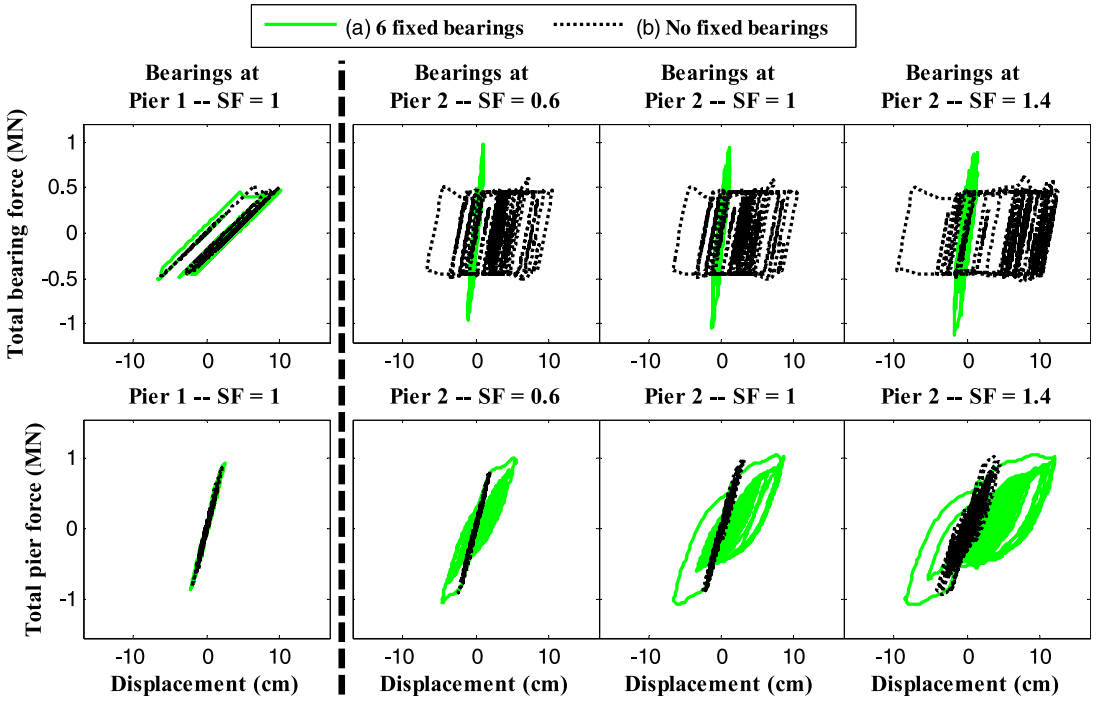

Fig. 15. Hysteretic behavior of bearings and bridge piers for different hazard levels

elastic deformations. For Pier 2, however, the response is highly dependent on the number of bearings with anchor bolts installed. The case where all six bearings have positive anchorage experiences no fusing in the bearing, thereby causing damage to the pier even for small hazards, whereas the cases with zero (or even two) anchored fixed bearings experience sliding of the bearings and essentially elastic behavior at the pier.

When the maximum response for each ground motion within the suite is averaged at the reference hazard level (SF = 1), the drift ratio for the pier supporting fixed bearings for the case in Fig. 15(a) is moderate at 1.8% and results in relatively high ductility demands $\mu = (\Delta_u - \Delta_y)/\Delta_y = 5$. As the number of bearings with anchorage decreases, the average pier drift ratio falls to about 25% of the drift ratio with all bearings anchored to the pier. Despite bearing configurations having a large influence on the local pier and bearing behaviors, these changes have little influence on the global bridge behavior, largely because of the influence of the abutment backwall and backfill. The abutment backwall and backfill limit longitudinal displacements to less than 20 cm (8 in.), even for large seismic hazard demands. At these displacements, the soil requires considerable energy to induce additional displacement. Consequently, when force demands are transferred from the pier with fixed bearings to the backwalls and backfill, the induced additional peak superstructure displacement is negligible.

Summary and Conclusions

Analytical models were developed to explore the response characteristics of bridges accounting for typical design practice in Illinois and incorporating quasi-isolated characteristics in the form of transverse restraints secured by steel anchors into concrete, large shear deformations of elastomeric bearings, and ultimately sliding of elastomers-on-concrete or PTFE-on-stainless steel. The models also included steel low-profile fixed bearings, with steel anchors into concrete substructures. Both fixed bearings and elastomeric bearings were intended to act as fuses to provide a force limitation so that substructures could be protected from large inelastic demands during a design earthquake, and instead, energy would be dissipated primarily through sliding at the interfaces of bearings and substructures. The primary deviation from the desired response was seen in the demands transmitted through the fixed bearings.

Experiments were carried out with steel fixed bearings, in longitudinal and transverse orientations, for two fusing mechanisms: weak anchors at the connection of the bottom plate to the concrete, and weak pintles at the connection of the top and bottom steel bearing plates. The weak anchors option was seen to be the preferable design option. In both the longitudinal and transverse orientations, the weak anchor ultimate anchor capacities corresponded to pure shear failures of the anchor material, with little localized damage to the surrounding concrete. Bearing response for the weak anchor designs was seen to be generally insensitive to loading orientation, and bidirectional response is therefore anticipated to be consistent with the responses observed for the two orthogonal tested orientations. For the weak pintles option, only the longitudinal orientation was limited by pintle failure, and even in that case, one of the anchors failed prior to the first pintle failure. In the transverse orientation with a weak pintles design, both anchors failed, and both pintles remained intact (although plastically deformed). Furthermore, the anchor failures for the transverse weak pintles case were below the top layer of steel reinforcing in the concrete, rather than at the concrete surface as the weak anchors design case had been. The capacity and mechanistic transition to the fused state was less reliably predicted for the weak pintles case and includes localized concrete crushing failures both before and after ultimate capacity is reached.

The weak anchors option exhibited reasonably predictable fuse capacity, accounting for a 0.6 factor for shear, a 0.8 factor for threads, and a friction coefficient of approximately 0.3 at the interface of the bottom steel plate on an elastomeric leveling pad. Primary uncertainties influencing the fuse capacity of weak anchor designs were installation procedures, which would tend to reduce capacity by unevenly loading individual anchors, and material strength uncertainty, which would tend to increase capacity when material suppliers provide higher strength material grades than specified. The uncertainty originating from installation procedures can be minimized by specifying that anchors be cast-in or that excess injected epoxy should be removed prior to installing masonry plates. Alternatively, if installation of anchors with similar relative positions in masonry plate holes is believed to be too difficult to enforce, design procedures should anticipate that the fixed bearing fuse capacity could range from that available with only one anchor engaged to that with both anchors engaged to bracket both peak load and peak displacement demands. On the basis of coupon tests for the supplied anchors, the material provided to meet a request for Grade 36 had strength approaching the upper limit of acceptability for Grade 36 material and slightly less than Grade 55. Practitioners should bear in mind that rejected Grade 55 material may be provided by contractors in place of requested Grade 36 material. Discussions with members of the IDOT Technical Review Panel for this research project indicated that it is not uncommon for higher strength material to be supplied in lieu of the actual specified material. Designers should anticipate that supplied materials may have a wide margin of overstrength, particularly in areas where seismic design has not historically been a governing design consideration. Designs attempting to capitalize on the benefits of a quasi-isolated system should either include accompanying project specifications to enforce strict control standards with sampling and testing procedures used in construction, or the bridge must be designed accounting for bounding characteristics of maximum force demand throughout the bridge with high anchor material strength and maximum sliding displacements and potential for unseating with low anchor material strength.

The key aspects that determined the effectiveness of the quasi-isolation performance were the anchorage of fixed bearings to the supporting pier cap and accounting for the presence of backfill at the abutments. Analyses indicated that inelastic demands at the pier supporting fixed bearings could be significantly reduced, and possibly even eliminated, for a design earthquake by selectively providing anchorage. When the bridge was floating, with no direct anchorage at fixed bearings (friction resistance only), the pier demand was unlikely to reach its yield capacity for a design earthquake. The reduced demand acting through the fixed bearings with fewer anchored bearings was balanced by increased force transferred to the abutment backfill, with a negligible difference in the overall bridge deck displacement. However, it should be noted that backfill effectiveness in arresting seismically induced superstructure motion was determined relying primarily on calibration of the analytical modeling components to a limited set of experimental data. Further investigation of backfill response is warranted, in consideration of its significance when investigating global bridge response. Regardless, failure to consider the backwall and backfill in analyses are certain to result in overestimations of system displacements and imply greater sensitivity of peak displacements to the omission of fixed bearing anchorage than is likely.

Acknowledgments

This article is based on the results of ICT R27-70: "Calibration and Refinement of Illinois' Earthquake Resisting System Bridge Design Methodology." ICT R27-70 was conducted in cooperation with the Illinois Center for Transportation (ICT); IDOT, Division of

Highways; and the U.S. DOT, Federal Highway Administration (FHWA). The contents of this article reflect the view of the authors, who are responsible for the facts and the accuracy of the data presented herein. The contents do not necessarily reflect the official views or policies of ICT, IDOT, or FHWA. The authors thank the members of the project Technical Review Panel, chaired by D. H. Tobias of IDOT, for valuable assistance with this research.

References

AASHTO. (2004). "Steel bridge bearing design and detailing guidelines." *SBB-1*, Washington, DC.

AASHTO. (2010a). *Guide specifications for seismic isolation design*, Washington, DC.

AASHTO. (2010b). *LRFD bridge design specifications*, Washington, DC.

AASHTO. (2011). *Guide specifications for LRFD seismic bridge design*, Washington, DC.

ASTM. (2007). "Standard specification for anchor bolts, steel, 36, 55, and 105-ksi yield strength." *F1554-07a*, West Conshohocken, PA.

Fernandez, J. A., and Rix, G. J. (2006). "Soil attenuation relationships and seismic hazard analyses in the Upper Mississippi Embayment." *Proc., 8th National Conf. on Earthquake Engineering*, Earthquake Engineering Research Institute, Oakland, CA, Paper No. 521.

Filipov, E. T. (2012). "Nonlinear seismic analysis of quasi-isolation systems for earthquake protection of bridges." M.S. thesis, Univ. of Illinois at Urbana–Champaign, Urbana, IL.

Filipov, E. T., et al. (2012). "Sensitivity of quasi-isolated bridge seismic response to variations in bearing and backwall elements." *Proc., 15th World Conf. on Earthquake Engineering*, International Association for Earthquake Engineering (IAEE), Tokyo, Paper No. 2978.

Filipov, E. T., et al. (2013a). "Seismic performance of highway bridges with fusing bearing components for quasi-isolation." *Earthquake Eng. Struct. Dynam.*, 42(9), 1375–1394.

Filipov, E. T., Fahnestock, L. A., Steelman, J. S., LaFave, J. M., Hajjar, J. F., and Foutch, D. A. (2013b). "Evaluation of quasi-isolated seismic bridge behavior using nonlinear bearing models." *Eng. Struct.*, 49, 168–181.

Illinois DOT (IDOT). (2007). *Standard specification for road and bridge construction*, IDOT, Springfield, IL.

Illinois DOT (IDOT). (2009). *Bridge manual*, IDOT, Springfield, IL.

LaFave, J., et al. (2013a), "Experimental investigation of the seismic response of bridge bearings." *Research Rep. No. FHWA-ICT-13-002*, Illinois Center for Transportation, Univ. of Illinois at Urbana–Champaign, Urbana, IL.

LaFave, J., et al. (2013b). "Seismic performance of quasi-isolated highway bridges in Illinois." *Research Rep. No. FHWA-ICT-13-015,* Illinois Center for Transportation, Univ. of Illinois at Urbana–Champaign, Urbana, IL.

Mander, J. B., Kim, D.-K., Chen, S. S., and Premus, G. J. (1996). "Response of steel bridge bearings to reversed cyclic loading." *National Center for Earthquake Engineering Research Rep. No. NCEER-96-0014*, Dept. of Civil Engineering, State Univ. of New York, Buffalo, NY.

McKenna, F., Mazzoni, S., and Fenves, G. L. (2006). *Open system for earthquake engineering simulation (OpenSees)*, Univ. of California, Berkeley, CA.

Steelman, J. S., Fahnestock, L. A., Filipov, E. T., LaFave, J. M., Hajjar, J. F., and Foutch, D. A. (2013). "Shear and friction response of non-seismic laminated elastomeric bridge bearings subject to seismic demands." *J. Bridge Eng.*, 10.1061/(ASCE)BE.1943-5592.0000406, 612–623.

Tobias, D. H., Anderson, R. E., Hodel, C. E., Kramer, W. M., Wahab, R. M., and Chaput, R. J. (2008). "Overview of earthquake resisting system design and retrofit strategy for bridges in Illinois." *Pract. Period. Struct. Des. Constr.*, 10.1061/(ASCE)1084-0680(2008)13:3(147), 147–158.